JOURNAL OF BACTERIOLOGY, Jan. 2006, p. 223–230 Vol. 188, No. 1
0021-9193/06/$08.00+0 doi:10.1128/JB.188.1.223–230.2006

The AidB Component of the *Escherichia coli* Adaptive Response to Alkylating Agents Is a Flavin-Containing, DNA-Binding Protein†

Mukta S. Rohankhedkar,[1] Scott B. Mulrooney,[2] William J. Wedemeyer,[3,4] and Robert P. Hausinger[1,2,3]*

Cell and Molecular Biology Program,[1] Department of Microbiology and Molecular Genetics,[2] Department of Biochemistry and Molecular Biology,[3] and Department of Physics,[4] Michigan State University, East Lansing, Michigan 48824-4320

Received 3 August 2005/Accepted 4 October 2005

Upon exposure to alkylating agents, *Escherichia coli* increases expression of *aidB* along with three genes (*ada*, *alkA*, and *alkB*) that encode DNA repair proteins. In order to begin to identify the role of AidB in the cell, the protein was purified to homogeneity, shown to possess stoichiometric amounts of flavin adenine dinucleotide (FAD), and confirmed to have low levels of isovaleryl-coenzyme A (CoA) dehydrogenase activity. A homology model of an AidB homodimer was constructed based on the structure of a four-domain acyl-CoA oxidase. The predicted structure revealed a positively charged groove connecting the two active sites and a second canyon of positive charges in the C-terminal domain, both of which could potentially bind DNA. Three approaches were used to confirm that AidB binds to double-stranded DNA. On the basis of its ability to bind DNA and its possession of a redox-active flavin, AidB is predicted to catalyze the direct repair of alkylated DNA.

Two general classes of environmental and laboratory chemicals are known to alkylate DNA. S_N1 reagents (e.g., methylnitrosourea and *N*-methyl-*N*′-nitro-*N*-nitrosoguanidine [MNNG]) react primarily with the N^7 and O^6 positions of guanine, N^3 of adenine, O^6 or O^4 of pyrimidines, and the nonphosphodiester oxygen atoms of the phosphate backbone. In contrast, S_N2 agents (e.g., methyl methanesulfonate and dimethylsulfate) react primarily with the N^1 position of adenine and N^3 of cytosine (40). Microorganisms generate endogenous methylation compounds, such as *S*-adenosylmethionine, and are exposed to exogenous methylating substances that can modify their DNA, RNA, and other cellular components.

To overcome the mutagenic and toxic effects of DNA methylation, *Escherichia coli* possesses a variety of DNA repair enzymes, some of which are induced as part of the "adaptive response to alkylating agents" (40, 43–46). A key component of this process is the Ada protein, associated with three distinct activities. The amino-terminal domain of Ada catalyzes a methyl phosphotriester methyltransferase reaction that repairs methyl phosphotriesters in the DNA backbone while irreversibly methylating its Cys-38 side chain. Similarly, the carboxyl-terminal domain of Ada possesses 4-methyl-T and 6-methyl-G methyltransferase activities that irreversibly methylate Cys-321. In addition to the single-turnover reactions catalyzed by Ada, the protein (in its Cys-38-methylated form) functions as an activator that enhances transcription of its own gene as well as those encoding AlkA, AlkB, and AidB. AlkA is a 3-methyl-A DNA glycosylase that removes the alkylated base to create abasic sites in the DNA product. AlkB is an Fe(II)- and α-ketoglutarate-dependent hydroxylase that uses oxidative demethylation chemistry to reverse methylation damage to 1-methyl-A and 3-methyl-C (42). In contrast to the situation for Ada, AlkA, and AlkB, the role of AidB in the adaptive response process remains uncharacterized.

The AidB sequence reveals a close relationship to acyl-coenzyme A (CoA) dehydrogenases, and crude cell extracts overproducing the protein exhibit isovaleryl-CoA dehydrogenase activity (22). Overexpression of *aidB* leads to reduced levels of mutagenesis caused by MNNG exposure (22), but the mechanism of protection against mutation is unknown. Curiously, some derivative strains with the gene insertionally inactivated exhibit enhanced tolerance to a methylating agent (45). This surprising result might be due to enhanced activity or stabilization of the protein in these constructs where the sites of insertion are localized to the 3′ region of the gene. While many questions about its function remain, AidB has been hypothesized to repair unidentified DNA lesions or to detoxify certain S_N1 reagents (22, 23).

As a first step to defining its role, we purified AidB and characterized several of its biophysical properties. We established that AidB is a flavin-containing protein with weak isovaleryl-CoA dehydrogenase activity. We generated a homology model of AidB based on the structure of a four-domain acyl-CoA oxidase, revealing a positively charged groove connecting the active sites and a second canyon of positive charges. These features represent potential DNA-binding sites. Significantly, we demonstrated that AidB binds to double-stranded DNA (dsDNA), which protects a large region of the protein from proteolysis. These studies set the stage for future efforts to characterize the function of AidB.

* Corresponding author. Mailing address: Microbiology and Molecular Genetics, 6193 Biomedical Physical Sciences, Michigan State University, East Lansing, MI 48824-4320. Phone: (517) 355-6463, ext. 1610. Fax: (517) 353-8957. E-mail: hausinge@msu.edu.

† Supplement material for this article may be found at http://jb.asm.org/.

MATERIALS AND METHODS

Cloning and expression of *aidB*. The *aidB* gene of *E. coli* K-12 (22) was amplified from host DNA by using the forward and reverse primers *aidB-Nco*-F 5′-AGG ATA TAC CAT GGA GGG AGA CAC AGT GCA C-3′ (introducing

an NcoI site at the 5′ end of the gene; the start codon is underlined) and *aidB-Hin*d-R 5′-TCT CGT AGA AGC TTT TAC ACA CAC ACT CCC CCC G-3′ (which introduces a HindIII site at the 3′ end of the gene). The amplified gene was digested with NcoI and HindIII and subcloned into the NcoI and HindIII sites of a pET28a vector (Novagen) to create pET28aAidB. This plasmid was transformed into *E. coli* C41[DE3] (33) that was grown on Luria-Bertani agar plates containing kanamycin (50 μg/ml), and the construct was confirmed to be correct by analyzing the NcoI and HindIII digestion products on a 1% agarose gel and by DNA sequencing. Cultures were grown overnight at 37°C with constant shaking at 200 rpm, and 1 ml was used to inoculate 1 liter of Terrific Broth (TB) medium (Fisher Biotech) containing kanamycin (50 μg/ml). Cells were grown at 37°C to an optical density at 600 nm of ~0.4, following which isopropyl-β-D-thiogalactopyranoside (IPTG) was added (final concentration of 2 mM), and the cultures were allowed to grow overnight. Cells were harvested by centrifugation, resuspended in 30 ml lysis buffer [10 mM Tris, pH 7.8, containing 1 mM EDTA, 0.3 M NaCl, 20% glycerol, 2 mM Tris(2-carboxyethyl)phosphine hydrochloride (TCEP; Pierce Biotechnology, Rockford, IL) as reductant, and 0.5 mM phenylmethylsulfonyl fluoride to prevent proteolysis], disrupted by sonication, and centrifuged at 27,000 × *g* for 2 h at 4°C.

Purification of AidB. The cell extracts were treated by using stepwise increasing concentrations of ammonium sulfate at room temperature, with each addition followed by centrifugation at 6,000 × *g* at 4°C to pellet the precipitated protein. The pellet resulting from the 30 to 45% ammonium sulfate treatment was dissolved in buffer A (10 mM Tris, pH 7.8, 1 mM EDTA, 20% glycerol, 2 mM TCEP) containing 1 M NaCl, and the soluble proteins were applied to a phenyl-agarose column (Sigma, St. Louis, MO) equilibrated in the same buffer. Contaminating proteins were eluted by washing the column with buffer A lacking NaCl, and AidB was eluted with buffer A containing 0.4% (wt/vol) deoxycholate. Fractions were analyzed by sodium dodecyl sulfate-polyacrylamide gel electrophoresis (SDS-PAGE) using a 10% running gel (21). The fractions containing the protein of interest were pooled, applied to a DEAE Sepharose column equilibrated in buffer A, and eluted with a linear gradient from buffer A to 1 M NaCl in buffer A containing 0.02% Triton X-100. Fractions were analyzed by SDS–10% PAGE.

Native molecular mass of AidB. Size exclusion chromatography was performed by using a Protein-Pak 300SW [diol(OH), 10 μm; 7.5 mm by 300 mm] column equilibrated in buffer containing 10 mM Tris, pH 7.8, 0.3 M NaCl, and 10% glycerol at 1 ml/min. The molecular mass of the native protein was estimated by comparing its retention time (monitored at 214 or 280 nm) to those of molecular mass standards (thyroglobulin, 670,000 Da; bovine γ-globulin, 158,000 Da; chicken ovalbumin, 44,000 Da; equine myoglobin, 17,000 Da; vitamin B_{12}, 1,350 Da; Bio-Rad).

Characterization of the AidB cofactor. Spectrophotometric quantification of the chromophore in AidB was carried out after denaturing the protein in 1% SDS. For cofactor identification, the intact AidB protein was applied to a matrix containing 2,5-dihydroxybenzoic acid and matrix-assisted laser desorption ionization (MALDI)–mass spectrometric (MS) analysis was performed by using the Applied Biosystems Voyager System 4148. The observed *m*/*z* ratio was compared to that for an authentic standard of flavin adenine dinucleotide (FAD) (11).

The effects of chemical reduction on the UV-visible spectra of free and protein-bound FAD cofactor (26 μM) were assessed by titrating samples (purged with nitrogen gas) with dithionite in an anaerobic cuvette while monitoring the absorbance (300 nm to 600 nm) with a Beckman DU 7500 or Hewlett-Packard HP8453 spectrophotometer. The concentration of dithionite used in this assay was quantified by monitoring the absorbance changes during analogous titration of protein-free FAD. Photoreduction of the flavin of AidB (8 μM subunit) was carried out by exposing an anaerobic sample (in buffer A containing 15 mM EDTA, 0.3 M NaCl, and 0.185 μM 5-deazaflavin; the latter was generously provided by Dave Arscott, Sumita Chakraborty, and Vincent Massey) to a 100-W halogen light (Philips narrow spot) source at a distance of 8.5 cm and at 0°C. The absorbance spectrum (300 nm to 600 nm) was monitored every 5 min by using a Beckman DU 7500 spectrophotometer. Fluorescence spectra were acquired using a Perkin-Elmer Luminescence spectrometer (model LS-50B).

Changes to the absorbance spectra of oxidized and fully reduced AidB protein were examined in the presence of 1 mM CoA, 1 mM butyryl-CoA, 1 mM isovaleryl-CoA, or 100 mM MNNG. In addition, the absorbance spectrum of oxidized protein was monitored upon addition of 5 mM sodium sulfite, 100 μM NADH, 15 mM nitroethane, 200 μM 5-methylcytosine, 200 μM 7-methylguanine, or 200 μM 5-methyl-2-deoxycytidine. Finally, the effect on AidB cofactor fluorescence was examined for protein in the presence of 10 μg/ml of a randomly chosen 29-mer of dsDNA.

Isovaleryl-CoA dehydrogenase activity assay. Isovaleryl-CoA dehydrogenase activity assays were performed essentially as described previously (8) but omitting the phenazine methosulfate mediator and reductant. Assays were carried out at room temperature in 200 mM phosphate buffer, pH 8.0, and using purified recombinant protein that had been dialyzed to remove TCEP. Isovaleryl-CoA was synthesized as previously described (38) or was purchased (Sigma). For routine assays, 2 mM isovaleryl-CoA was used as the substrate and 0.1 mM 2,6-dichlorophenolindophenol (DCPIP) was used as the terminal electron acceptor in a final volume of 300 μl. The change in absorbance at 600 nm was monitored by using a Beckman DU 7500 spectrophotometer, and the enzyme activity was calculated by assuming an extinction coefficient of 20.6 mM^{-1} cm^{-1} for DCPIP (8).

DNA binding assays. The ability of AidB to bind to DNA was assessed by three independent approaches. For one method, AidB (5 to 450 μg) was applied to columns of dsDNA-cellulose (200 μg calf thymus DNA per ml of resin; 1.0 cm by 10 cm; Sigma) equilibrated in buffer A (except that TCEP was replaced by dithiothreitol), pH 8.0, and the columns were washed in a stepwise manner with buffer solutions containing 0, 0.1, 0.5, and 1.0 M NaCl (5). Fractions eluting from the column were examined for AidB by SDS-PAGE.

A second technique to assess DNA binding by AidB focused on the ability of bound DNA to protect AidB from proteolysis. Linearized pCAT DNA (Novagen) (200 ng) was incubated with 50 μg of purified AidB in 20 μl buffer (20 mM Tris, 1 mM EDTA, pH 7.8) for 1 h at 37°C, chymotrypsin (Sigma) was added (1:20 [wt/wt], protease:AidB), samples were incubated at 37°C for 0, 3, or 6 h, and the reactions were quenched by adding 0.3 volumes of 8% trichloroacetic acid followed by incubation on ice. The extent of proteolysis and sizes of the resulting AidB fragments were identified by SDS-PAGE using gels comprised of 18% polyacrylamide. The proteolytically derived peptides were electroblotted (50 V for 3 h at 4°C) onto a polyvinylidene difluoride membrane using transfer buffer containing 10% methanol and 10 mM CAPS [3-(cyclohexylamino)-1-propanesulfonic acid], pH 11 (31). After staining with 0.1% Coomassie R-250 in 40% methanol for 45 s to identify the location of the desired band, the membrane was destained with several changes of 50% methanol and rinsed with water. The amino-terminal sequence of the desired AidB fragment was obtained at the MSU Macromolecular Structure, Sequencing, and Synthesis Facility by using an Applied Biosystems Procise cLC 494 Protein/Peptide Sequencer.

As a third approach, aliquots of pUC19 DNA (200 ng; Novagen) were incubated with AidB (1 μM to 50 μM) in 10 μl buffer A at 37°C for 30 min before being electrophoresed in a 1% agarose gel using 40 mM Tris, pH 7.8, 1 mM EDTA buffer, as previously described (14). To probe the ability of AidB to bind to methylated DNA, pUC19 DNA was methylated by incubating it with 10 mM MNNG at 30°C for 1 h. The methylated plasmid DNA was purified by using spin columns (QIAGEN) to remove excess MNNG and examined for interaction with AidB as described above. In some cases, the plasmid was treated with restriction enzymes prior to incubation with AidB.

Sequence analysis and homology modeling. The full-length sequence of AidB was submitted to the Bioinfo.pl Meta Server (http://bioinfo.pl/Meta/) hosted by the BioinfoBank Institute of Poland (10). Secondary-structure predictions were carried out by using the four best-validated (19) secondary-structure servers, PsiPRED (15, 32), SABLE2 (1), SAM-T2K (16), and PROFsec (39). The results were parsed, formatted, and visualized using laboratory-written software that is publicly available on a web-server (http://proteins.msu.edu/Servers/Secondary_Structure/visualize_secondary_structure_predictions.html) and covered by the GNU General Public License.

PIR (protein information resource) alignments of full-length AidB to two parent structures, rat short chain acyl-CoA dehydrogenase (PDB accession code 1JQI) and rat liver peroxisomal acyl-CoA oxidase-II (PDB accession code 1IS2), were obtained from the PSI-BLAST (2) and FFAS03 (13) servers, respectively. These PIR alignments and the corresponding PDB files were converted into a homology model of AidB by using laboratory-written software that is publicly available on a web server (http://proteins.msu.edu/Servers/Homology_Modeling/construct_homolog_PDB.html) and covered by the GNU General Public License. Ribbon illustrations of the models were generated by using MOLMOL (20), and electrostatic potential analyses utilized GRASP (37).

RESULTS

Purification of AidB. *E. coli aidB* was amplified by PCR to yield the expected 1.7-kb fragment which was cloned into the NcoI-HindIII site of pET28a (Novagen) and transformed into *E. coli* C41[DE3] cells. Using TB medium, optimal production of AidB was observed following overnight growth at 37°C and using 2 mM IPTG (data not shown). Following sonication and

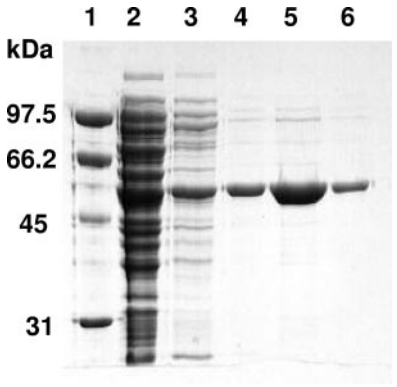

FIG. 1. SDS-PAGE analysis of AidB purification. AidB was isolated from extracts of *E. coli* C41[DE3] cells containing pET28aAidB by ammonium sulfate precipitation followed by successive chromatography using phenyl-Sepharose and DEAE-Sepharose columns. Fractions were analyzed by using SDS–10% PAGE. Lane 1, standards; lane 2, cell extracts; lane 3, 30 to 45% ammonium sulfate pellet dissolved in buffer A; lanes 4 and 5, phenyl-Sepharose fractions; lane 6, DEAE-Sepharose pooled fractions.

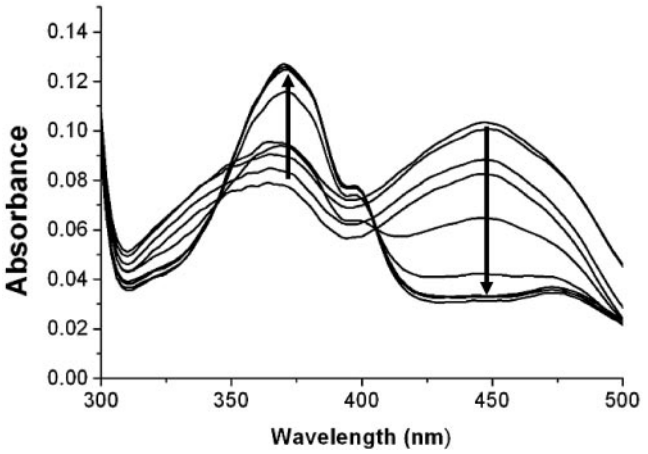

FIG. 2. Photoreduction of AidB. An anaerobic sample of AidB (~8 μM subunit concentration) was photoreduced by using a 100-W halogen lamp while monitoring changes in its spectrum at 5-min intervals. The final AidB spectrum corresponds to the one-electron-reduced flavin state.

centrifugation, cell extracts were treated with increasing concentrations of ammonium sulfate, and the desired protein was found to precipitate in the 30% to 45% fraction. The resolubilized sample was subjected to phenyl-Sepharose chromatography, with elution requiring low salt and inclusion of 0.4% (wt/vol) deoxycholate, to provide yellow fractions that contained a protein coinciding with the predicted molecular mass of 60,900 Da (Fig. 1). The pooled sample was purified to apparent homogeneity by DEAE-Sepharose chromatography in buffer that contained 0.02% Triton X-100 to enhance the protein stability. The typical yield was 30 mg of purified AidB per liter of culture. Purified protein was stored in this buffer at 4°C.

Biophysical characterization of AidB. On the basis of its retention time during size exclusion chromatography and comparison to standard proteins, AidB was estimated to possess a molecular mass of 200,000 ± 30,000 Da (data not shown). Given that the monomer molecular mass is predicted to be 60,591 Da, the sample is most consistent with a homotrimeric or homotetrameric quaternary structure.

AidB was examined for the presence of a flavin cofactor, suspected from the protein's distinctive yellow color and the known sequence homology to acyl-CoA dehydrogenases and oxidases. The absorbance spectrum of purified AidB exhibited major features at 460 and 370 nm, consistent with the presence of a flavin. A sample of AidB was treated with 1% SDS and heated for 5 min at 37°C to release the flavin; on the basis of the absorbance intensity at 460 nm and an FAD ε_{450} of 11,300 M^{-1} cm^{-1}, AidB was estimated to contain 0.92 mol of flavin per mol of subunit. Direct confirmation of the presence of FAD (as opposed to flavin mononucleotide or riboflavin) was obtained by MALDI-MS analysis that revealed a feature at *m/z* of 787.60 (data not shown), agreeing well with the calculated value of 785.16 for FAD (11). The FAD cofactor bound to AidB was examined for its fluorescence properties by scanning excitation wavelengths from 300 to 500 nm and measuring emission at 520 nm. No significant emission was detected, indicating that the fluorescence of the FAD is highly quenched when bound to the protein.

To further characterize the AidB-bound flavin, the protein was treated with the chemical reducing agent sodium dithionite in an anaerobic cuvette (data not shown). Titration of the enzyme with a solution of dithionite led to changes in the absorbance spectra that were consistent with three distinct phases. The first few additions of reductant did not affect the absorbance, presumably because residual oxygen was being consumed. Further addition of up to one equivalent of dithionite resulted in a steady decrease in absorbance at 450 nm and an increase in absorbance at 372 nm. Continued addition of dithionite resulted in a uniform decrease in absorbance across the spectrum, ending with the completely reduced form of protein-bound FAD. In contrast, titration of protein-free FAD with dithionite (used to quantify the concentration of the dithionite reductant) led to a monotonic conversion of the oxidized to the reduced flavin (spectra not shown). The intermediate observed during reduction of the protein corresponds to the stable, one-electron-reduced anionic semiquinone; formation of this stable species is characteristic of many flavoprotein oxidases (27). Unlike most flavin-containing oxidases (29), however, the protein did not react with added sulfite as shown by the lack of any spectroscopic change (data not shown).

In the presence of EDTA, free flavins are known to efficiently catalyze the photoreduction of a wide variety of flavoproteins (28, 30); thus, additional AidB flavin reduction studies were carried out using 5-deazaflavin and excess EDTA in the presence of light. Photoreduction of AidB for 30 min converted the enzyme-bound FAD to the anionic semiquinone state, but no additional changes were observed upon further incubation (Fig. 2). Although these conditions are highly artificial, the observations provide added support that the one-electron reduced form of the enzyme is stable, perhaps due to the presence of a positively charged side chain near the anionic N^1 of the flavin. The enzyme-bound flavin in both the semiquinone and fully reduced states was reoxidized upon incubation in the presence of oxygen.

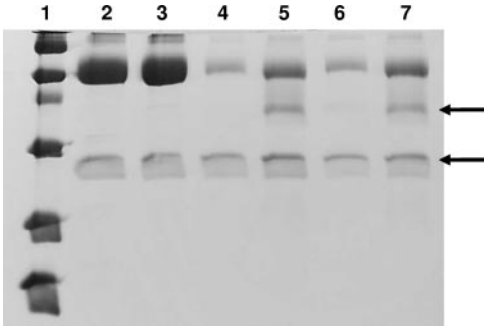

FIG. 3. DNA-induced protection against protease digestion of an AidB domain. AidB (50 μg) was digested with 2.5 μg of chymotrypsin for 0, 3, or 6 h in the absence of DNA (lanes 2, 4, and 6) or in the presence of 200 ng of plasmid DNA (lanes 3, 5, and 7) at 37°C. The reactions were quenched with trichloroacetic acid, and the samples were analyzed by SDS-PAGE on an 18% gel. Lane 1 contains molecular mass markers (97.4, 66.2, 45, 31, 21.5, and 14.4 kDa). The band designated by the upper arrow is the 50-kDa fragment that was subjected to Edman degradation, and the band shown by the lower arrow is chymotrypsin.

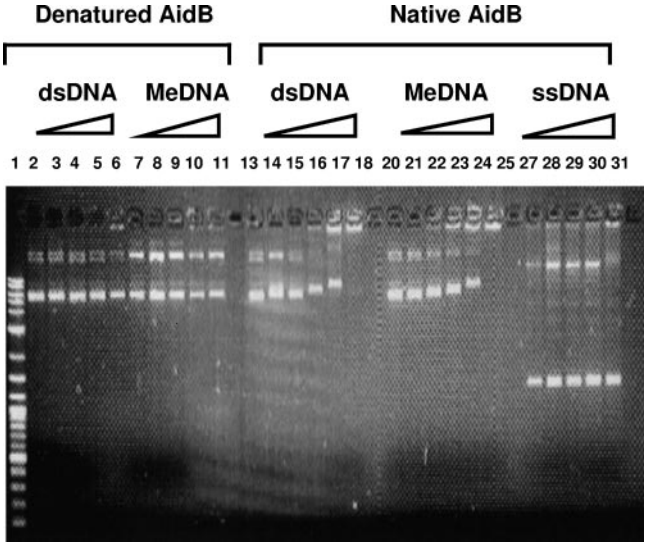

FIG. 4. AidB-induced mobility shift of dsDNA. Varied concentrations (0 μM, 0.1 μM, 0.5 μM, 0.75 μM, 1 μM, and 2 μM) of heat-denatured AidB (lanes 2 to 11) or native AidB (lanes 13 to 31) were incubated with nonmethylated dsDNA (lanes 2 to 6 and 13 to 18), methylated dsDNA (MeDNA) (lanes 7 to 11 and 20 to 25), and ssDNA (lanes 27 to 31) for 1 h at 37°C prior to analysis on a 1% agarose gel. The DNA samples included 200 ng pUC19 dsDNA (yielding the intense lower band of supercoiled plasmid and the slower-migrating relaxed species) or M13 phage ssDNA (showing the prominent lower band from circular ssDNA and the upper band of contaminating dsDNA) in 10 μl of buffer (pH 7.2). AidB was denatured by heating it to ~70°C for 5 min prior to incubation with DNA. Lane 1 shows the New England Biolabs 2-log DNA ladder as the standard.

Several other additives were examined for their effects on the AidB flavin spectrum. No perturbation of the visible spectrum was observed upon addition of NADH, sulfite (see above), CoA, butyryl-CoA, or isovaleryl-CoA to the oxidized enzyme. Similarly, neither the methylating agent MNNG nor nitroethane (a substrate for the flavoenzyme nitroalkane oxidase [35]) led to any changes in the FAD spectrum. CoA, butyryl-CoA, isovaleryl-CoA, and MNNG also failed to affect the spectrum of fully reduced enzyme (data not shown).

Enzymatic characterization of AidB. Using the artificial electron acceptor DCPIP, AidB was confirmed to possess low levels of isovaleryl-CoA dehydrogenase activity (0.0060 ± 0.0022 μmol min^{-1} [mg protein]$^{-1}$ when using 2 mM acyl-CoA substrate). The presence of DNA did not influence the level of dehydrogenase activity significantly. The finding of weak isovaleryl-CoA dehydrogenase activity despite the lack of spectral perturbation by isovaleryl-CoA can be rationalized by either a very weak affinity for this poor substrate or the presence of only a small population of protein molecules with this activity.

DNA binding by AidB. AidB was suspected to bind to DNA on the basis of its coregulation with DNA repair enzymes and because a short region of its C terminus was homologous to a DNA-binding region of topoisomerase I (see the next section). To further test this hypothesis, three approaches were used to evaluate whether AidB binds DNA. First, AidB was shown to be retained by a column of dsDNA-cellulose but could be eluted with 0.5 M NaCl (data not shown). Second, the presence of dsDNA was shown to protect a domain of AidB (~50 kDa) from digestion by chymotrypsin (with the protected domain and the protease indicated by arrows in Fig. 3). N-terminal sequencing of the protected fragment revealed an amino acid sequence of SNTTRAERLE, consistent with cleavage after residue Met-194 (predicted to be located in a flexible loop of the protein; see below) to produce a C-terminal fragment with the predicted size of 50,257 Da. Finally, gel band mobility shift studies demonstrated that AidB binds to dsDNA (Fig. 4). In these studies, the major band of starting material is the supercoiled plasmid and the slower-migrating species is the nicked plasmid; AidB appears to bind preferentially to the relaxed form. Remarkably, dsDNA-AidB interaction resulted in a shift of the dsDNA band to the top of the gel as if each protein molecule is capable of binding to multiple molecules of dsDNA and each DNA molecule binds several AidB proteins, resulting in aggregation. DNA retardation was not observed when using heat-denatured (~70°C for 5 min) AidB (lanes 2 to 11), and little interaction was noted when using single-stranded DNA (ssDNA) (lanes 27 to 31). Of potential functional significance, repeated experiments demonstrated that slightly lower concentrations of AidB were required to perturb the migration of MNNG-treated DNA (lanes 20 to 25) compared to nonmethylated samples (lanes 13 to 18). It should be noted, however, that the methylated DNA also contained a larger percentage of nicked DNA; thus, AidB may prefer to bind to the relaxed polymer. Consistent with the absence of precise DNA sequence specificity, AidB was shown to shift each of the bands arising from EarI digestion of pCAT plasmid DNA and to bind to a randomly selected 29-mer dsDNA oligomer (data not shown). In addition, methylated 29-mer dsDNA was bound more tightly than the nonmethylated oligomer according to mobility shifts in a 4 to 20% gradient polyacrylamide gel (data not shown).

Sequence analysis and homology modeling. Preliminary analysis using the Bioinfo.pl server showed that the N-terminal 440 residues of the 541-residue AidB are homologous to the acyl-CoA dehydrogenases (9), a family of enzymes that form

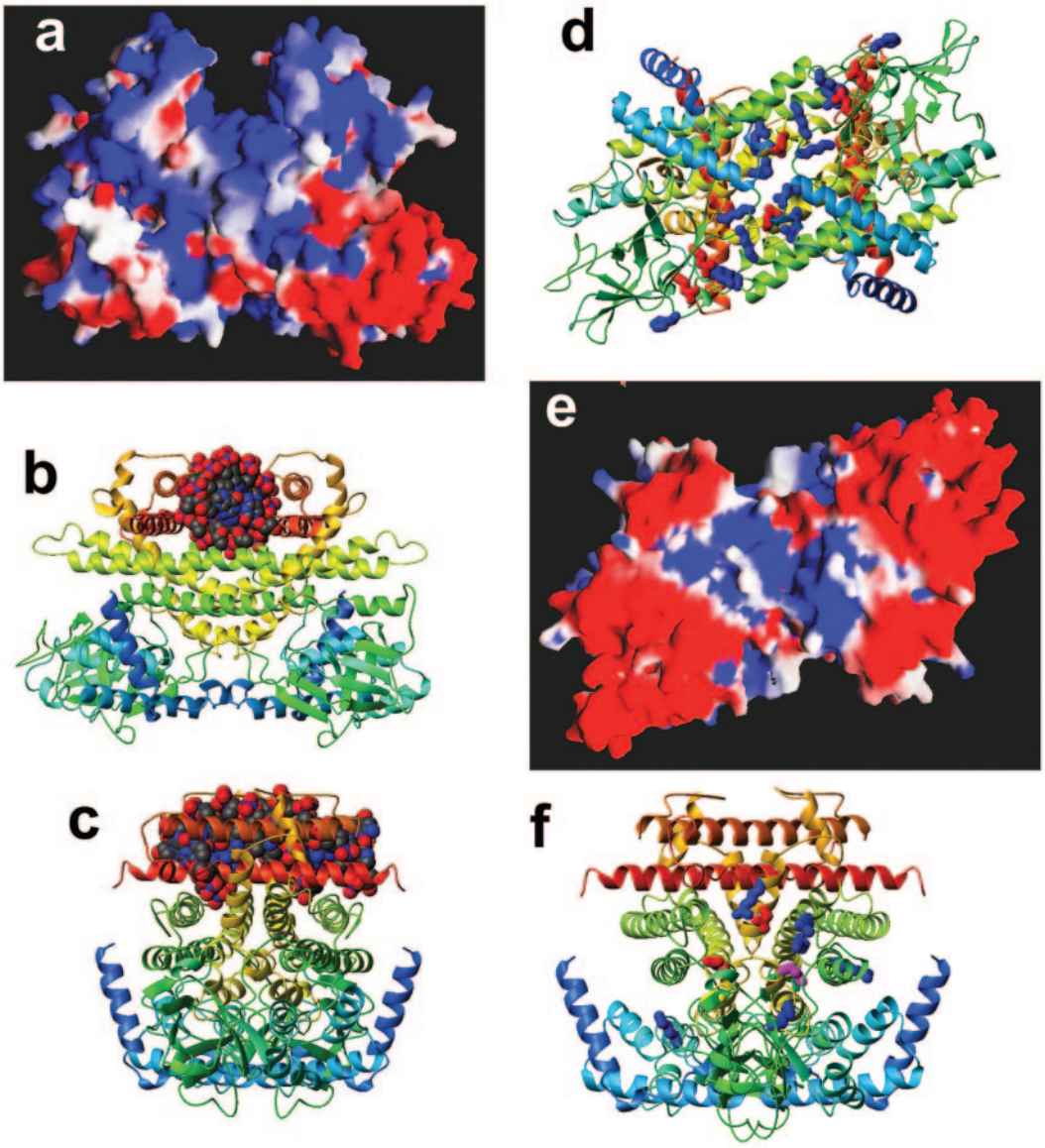

FIG. 5. Homology model of AidB. (a) An electrostatic potential analysis of the homodimer, with the positive charge in blue and negative charge in red, depicting a positively charged canyon created by the C-terminal region of the protein. (b) The same view shown as a ribbon diagram, with the chain color varying from blue to red progressing from the N to C terminus, with a dodecamer of B-form DNA manually positioned in the positively charged canyon at the top. (c) The same molecule rotated by 90° around a vertical axis. (d) Ribbon diagram of the homodimer as viewed after rotating the structure from panels a and b by ~90° around a horizontal axis. The canyon is now at the back of the molecule. A shallow groove is depicted with conserved positive residues shown in blue and conserved negative residues in red. (e) An electrostatic potential analysis of AidB in the same view. (f) Ribbon diagram of AidB as viewed in panel c with six conserved positively charged residues, three conserved negatively charged residues, and a conserved Cys, all located at the substrate-binding site of acyl-CoA dehydrogenases/oxidases, shown in blue, red, and yellow.

tightly bound homodimers or homotetramers and typically have three domains: an N-terminal α-helical domain, a middle β-sheet domain, and a C-terminal helical bundle (18). The dimeric structure of a related protein family member, rat liver peroxisomal acyl-CoA oxidase II (PDB accession code 1IS2), features a fourth helical domain (36). A consensus of secondary-structure servers agreed that the C-terminal 102 residues of AidB are α-helical and consistent with the 1IS2 structure (Fig. S1 in the supplemental material). Therefore, we made a homology model of the full-length AidB homodimer using 1IS2 as the parent structure (Fig. 5). This four-domain model is best understood after carrying out a detailed sequence comparison of AidB analogues to identify critical residues, as described below.

To identify full-length homologues of AidB (versus the many acyl-CoA dehydrogenases resembling only the three N-terminal domains), we submitted its C-terminal 102 residues to the NCBI PsiBLAST server (http://www.ncbi.nlm.nih.gov/BLAST). After seven rounds of PsiBLAST, no new homologues were identified above the E = 0.005 level. In all, PsiBLAST identi-

fied 57 homologues of AidB of similar lengths, 550 ± 13 residues (2σ deviation). These sequences, all annotated as putative acyl-CoA dehydrogenases, were filtered to remove sequences with greater than 90% identity, producing a nonredundant set of 34 homologous sequences. The closest hits were from two related enterobacteria, *Salmonella* and *Yersinia*, but hits were also identified from some γ-proteobacteria (*Pseudomonas*, *Idiomarina*, *Azotobacter*, and *Acinetobacter*), β-proteobacteria (*Burkholderia*, *Ralstonia*, *Chromobacterium*, *Azoarcus*, and *Bordetella*), α-proteobacteria (*Brucella*, *Bartonella*, *Rhodopseudomonas*, and various rhizobia), and even gram-positive bacteria (*Mycobacterium*, *Streptomyces*, *Nocardia*, and *Desulfitobacterium*).

The 34 nonredundant, full-length AidB-like sequences were aligned (Fig. S2 in the supplemental material) using the T-Coffee webserver (http://igs-server.cnrs-mrs.fr/Tcoffee/tcoffee_cgi/index.cgi), which is the best-validated multiple sequence alignment method (19). Despite the evolutionary distance between the organisms, AidB is highly conserved, with no less than 67 absolutely conserved residues (numbering is based on the *E. coli* AidB sequence): **Asn10**, **Ala62**, **Pro67**, **Gly76**, **Arg78**, **Pro86**, **Cys133**, **Pro134**, **Met137**, **Thr138**, **Lys175**, **Gly181**, Thr185, Glu186, **Lys187**, **Gln188**, **Gly189**, Gly190, **Asp192**, Ala200, **Gly212**, **His213**, Lys214, Phe216, **Ser218**, **Pro220**, Asp223, **Cys237**, **Phe238**, **Pro241**, **Asn250**, **Leu257**, **Lys258**, **Lys260**, Gly262, **Asn263**, **Asn266**, **Ser268**, **Glu270**, **Glu272**, **Gly282**, **Gly287**, **Met294**, **Thr298**, **Arg299**, **Arg311**, Arg324, Leu331, **Met337**, **Arg375**, Lys382, **Glu395**, **Glu398**, Gly401, **Gly402**, Gly404, **Arg413**, **Glu417**, **Pro419**, **Trp424**, Glu425, Gly426, **Gly428**, **Asn429**, **Asp434**, **Arg437**, and **Arg483**. The residues shown in boldface are identical in AidB-like sequences but not highly conserved among the non-AidB-like homologues; residues in normal typeface are nearly universally found, or conservatively replaced, in the entire group of acyl-CoA dehydrogenases. In addition, five charges are conserved absolutely: **Glu128**, **Asp166**, **Arg242**, **Glu407** and **Arg416**, again with boldface indicating that all five are conserved in the AidB-like homologues but not in non-AidB-like acyl-CoA dehydrogenases. The absolutely conserved residue Glu425 corresponds to the catalytic glutamate in most of the short- and medium-chain acyl-CoA dehydrogenases. Of interest, this residue is an alanine in human isovaleryl-CoA dehydrogenase that uses Glu254 as the general base, whereas AidB **Thr298**, absolutely conserved in AidB-like sequences, corresponds to the catalytic glutamate found in the long-chain acyl-CoA and isovaleryl-CoA dehydrogenases. The conservation of Glu425 suggests that a dehydrogenase or oxidase activity is essential to the physiological function of AidB.

The homodimer structure (Fig. 5) has three noteworthy features that may pertain to the function of AidB. First, there is a prominent "canyon" composed mainly of the C-terminal helical hairpin stacked across similarly long helices of the third domain. The canyon has a strong positive electrostatic potential (Fig. 5a) and has the correct dimensions (~20 Å wide, ~20 Å deep, and ~40 Å long) to accommodate a 12-bp stretch of dsDNA, as illustrated by the models (Fig. 5b and c) that include a Dickerson-Drew dodecamer of B-form DNA (6). This domain also exhibits weak similarity (17 identities over 47 AidB residues) to a DNA-binding domain of human topoisomerase I (data not shown), further supporting our hypothesis that dsDNA binds to this region of AidB. Second, the opposite face has a more shallow groove lined with conserved positive charges from both subunits, specifically, **Arg78**, **Lys187**, **His213**, **Lys258**, and **Lys260** from one subunit and Arg324, **Arg413**, and **Arg416** from the other (16 blue side chains in Fig. 5d). Of these residues, only Arg324 is widely distributed in non-AidB-like acyl-CoA dehydrogenases. There is one conserved negative charge in the center of the groove (**Glu407**) and two (**Glu270**, **Glu272**) on its periphery (six red side chains in Fig. 5d), with these residues not well conserved in non-AidB-like sequences. The electrostatic potential of this region is generally positive (Fig. 5e), consistent with this symmetric groove being a secondary DNA binding site. This groove is oriented at approximately 45° relative to the putative DNA-binding canyon described above. Third, the catalytic substrate binding site also is lined with conserved positive charges (blue side chains in Fig. 5f), namely, Lys214, **Arg242**, **Arg299**, **Arg375**, Lys382, and **Arg437** (all from the same subunit), three conserved negative charges (**Asp192**, **Asp434**, and the catalytic Glu425, shown as red side chains in Fig. 5f), and a conserved cysteine residue, **Cys237** (shown in yellow in Fig. 5f). Only three of these residues (Lys214, Lys382, and Glu425) are conserved beyond the AidB-like sequences.

AidB can be aligned with acyl-CoA dehydrogenases that form homotetramers, such as isovaleryl-CoA dehydrogenase (18), from which a tetrameric model of AidB could be constructed. However, the tetramerization interface of these enzymes coincides with the predicted location of the C-terminal helices that we have suggested form a DNA-binding "canyon." Therefore, we cannot reliably propose such a homotetramer model.

DISCUSSION

Characterization of AidB as a flavin-containing protein with spurious isovaleryl-CoA dehydrogenase activity. The results described above present the first reported purification of AidB, a component of the *E. coli* adaptive response to alkylating agents. Consistent with expectations based on sequence comparisons and in agreement with the observed activity in crude cell extracts (22), purified AidB is a flavin-containing enzyme with isovaleryl-CoA dehydrogenase activity. Curiously, AidB possesses a Glu residue (position 425) at the position of the active-site carboxylate base found in most acyl-CoA dehydrogenases, whereas human isovaleryl-CoA dehydrogenase possesses an Ala at this position and utilizes a Glu on a distinct helix as its general base (18). The level of isovaleryl-CoA dehydrogenase activity observed in AidB is quite low compared to other acyl-CoA dehydrogenases. For comparison, human isovaleryl-CoA dehydrogenase exhibits 8.2 to 11.7 μmol min^{-1} $(mg\ protein)^{-1}$ under similar conditions or >1,000-fold-higher activity (3, 34). In addition, human butyryl-CoA dehydrogenase (7), human glutaryl-CoA dehydrogenase (25), and various rat acyl-CoA dehydrogenases (12) exhibit specific activities of 7.4 to 15.3 μmol min^{-1} $(mg\ protein)^{-1}$ using this assay. We conclude that isovaleryl-CoA dehydrogenase activity in AidB is a side reaction that is distinct from its functional role.

Identification of AidB as a DNA-binding protein. We demonstrated that AidB binds to dsDNA-cellulose, is protected

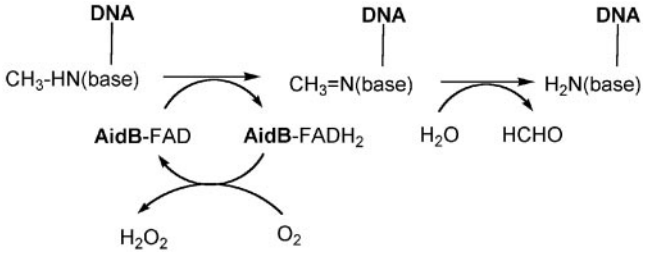

FIG. 6. Hypothetical function of AidB. On the basis of its FAD cofactor and its ability to bind to methylated DNA, AidB might function as a methylated base dehydrogenase. The Schiff's base product would hydrolyze to release the free base plus formaldehyde, and the reduced flavin could either react with oxygen to produce hydrogen peroxide (as shown) or transfer electrons to another suitable electron acceptor. Analogous chemistry is possible for demethylation of bases alkylated at certain oxygen atoms.

from proteolysis by added dsDNA, and causes a mobility shift of dsDNA bands in native gels. This interaction between AidB and dsDNA was quite surprising, given the sequence homology of AidB to acyl-CoA dehydrogenases, but is compatible with AidB possessing a methylated dsDNA repair activity. No sequence specificity was observed when examining large plasmid fragments, but further studies are warranted to characterize this in greater detail.

Quaternary structure of AidB. The gel-permeation chromatographic properties of AidB are consistent with a trimeric or tetrameric quaternary structure, but on the basis of its structural relationships to acyl-CoA dehydrogenases/oxidases (which are all found to be dimers or tetramers) (18), we conclude that AidB is most likely a tetramer. Thus, the homology model shown in Fig. 5 represents only half of the native size of the molecule. A less likely alternative is that AidB forms a homodimer with unstructured regions that cause the protein to have an unusually large hydrodynamic volume for its mass.

Predicted structure of AidB. Overall, AidB seems likely to adopt a four-domain fold similar to rat liver peroxisomal acyl-CoA oxidase II (1IS2). A homology model of an AidB homodimer using this parent structure reveals a groove of positively charged residues that are absolutely conserved among full-length AidB homologues but not among non-AidB-like acyl-CoA dehydrogenases. This groove connects the two putative active sites, which are themselves lined with absolutely conserved positive charges, a single cysteine (**Cys237**), and a glutamate that is necessary for catalysis in the structurally homologous short- and medium-chain acyl-CoA dehydrogenases. We propose that the groove binds ~20 bp of dsDNA, positioning it near the active sites. At least one acyl-CoA dehydrogenase family member binds to a large-molecule substrate; i.e., FkbI functions in FK520 biosynthesis and binds acylated acyl carrier protein (47).

Interestingly, the fourth domain of AidB (residues 440 to 541) in our homology model forms a deep "canyon" that seems likely to bind double-stranded DNA. This domain is poorly conserved, however, and dsDNA bound in this canyon would have difficulty in reaching the putative active site, requiring a sharp turn that is inconsistent with the known stiffness of dsDNA. This is true even for models of tetrameric AidB in which dsDNA bound in the canyon of one dimer could in principle bind in the active site of the other homodimer. These features lead us to hypothesize that the fourth domain does not directly influence catalysis but serves a structural role; e.g., a "scaffolding" that binds to DNA, stabilizes the relative position of the subunits in the homodimer, and, possibly, precisely positions the catalytic residues.

Potential cellular function of AidB. Although AidB's role in the cell remains unknown, the presence of an enzymatically active flavin and the protein's demonstrated DNA-binding capability suggests that AidB uses a dehydrogenase activity to repair alkylated DNA by a mechanism such as that shown in Fig. 6 (note that reoxidation of the reduced flavin is shown to occur by an oxygenase reaction, but electron donation to a separate electron carrier is another reasonable option). Several small molecules are known to be dealkylated by such oxidase mechanisms, including methylglycine (17), polyamines (24), and γ-*N*-methylaminobutyrate (4). In addition, a precedent for demethylation of methylated proteins by the LSD1 flavoenzyme, a methylated histone demethylase, was recently reported to use this mechanism (41). Alternatively, a flavin-dependent monooxygenase activity could be invoked to repair alkylation damage. Other potential roles are possible for AidB, such as prevention of DNA damage as seen in the case of the Dps protein (26). Further experiments to delineate the function of AidB are in progress. Interestingly, full-length AidB homologues are not detected in many bacteria closely related to *E. coli*, such as *Klebsiella*, *Vibrio*, *Shewanella*, and *Photorhabdus*, that possess other alkylation repair enzymes. The number of homologues of AidB seems to be far smaller than those of AlkA and AlkB. We also note that whereas *ada* and *alkB* form a transcriptional unit, *alkA* and *aidB* are well separated from this operon and from each other. These observations raise the possibility that AidB may be of secondary importance for repair of alkylation damage to DNA.

ACKNOWLEDGMENTS

We thank Leron Katsir for assistance with some of the homology modeling studies.

This work was supported by National Institutes of Health grant GM063584.

REFERENCES

1. **Adamczak, R., A. Porollo, and J. Meller.** 2005. Combining prediction of secondary structure and solvent accessibility in proteins. Proteins Struct. Funct. Genet. **59:**467–475.
2. **Altschul, S. F., T. L. Madden, A. A. Schaffer, J. H. Zhang, Z. Zhang, W. Miller, and D. J. Lipman.** 1997. Gapped BLAST and PSI-BLAST: a new generation of protein database search programs. Nucleic Acids Res. **25:** 3389–3402.
3. **Battaile, K. P., M. McBurney, P. P. Van Veldhoven, and J. Vockley.** 1998. Human long chain, very long chain and medium chain acyl-CoA dehydrogenases are specific for the S-enantiomer of 2-methylpentadecanoyl-CoA. Biochim. Biophys. Acta **1390:**333–338.
4. **Chirabau, C. B., C. Sandu, M. Fraaije, E. Schiltz, and R. Brandsch.** 2004. A novel γ-*N*-methylaminobutyrate demethylating oxidase involved in catabolism of the tobacco alkaloid nicotine by *Arthrobacter nicotinovorans* pAO1. Eur. J. Biochem. **271:**4677–4684.
5. **deHaseth, P. L., C. A. Gross, R. R. Burgess, and M. T. Record, Jr.** 1977. Measurement of binding constants for protein-DNA interactions by DNA-cellulose chromatography. Biochemistry **16:**4777–4783.
6. **Drew, H. R., R. M. Wing, T. Takano, C. Broka, S. Tanaka, K. Itakura, and R. E. Dickerson.** 1981. Structure of a B-DNA dodecamer: conformation and dynamics. Proc. Natl. Acad. Sci. USA **78:**2179–2183.
7. **Eder, M., F. Krautle, Y. Dong, P. Vock, V. Kieweg, J. J. Kim, A. W. Strauss, and S. Ghisla.** 1997. Characterization of human and pig kidney long-chain-acyl-CoA dehydrogenases and their role in beta-oxidation. Eur. J. Biochem. **245:**600–607.

8. **Engel, P. C.** 1981. Butyro-CoA dehydrogenase from *Megasphaera elsdenii*. Methods Enzymol. **71:**359–366.
9. **Ghisla, S., and C. Thorpe.** 2004. Acyl-CoA dehydrogenases. A mechanistic overview. Eur. J. Biochem. **271:**494–508.
10. **Ginalski, K., A. Elofsson, D. Fisher, and L. Rychlewski.** 2003. 3D-Jury: a simple approach to improve protein structure predictions. Bioinformatics **19:**1015–1018.
11. **Halada, P., C. Leitner, P. Sedmera, D. Haltrich, and J. Volc.** 2003. Identification of the covalent flavin adenine dinucleotide-binding region in pyranose 2-oxidase from *Trametes multicolor*. Anal. Biochem. **314:**235–242.
12. **Ikeda, Y., K. Okamura-Ikeda, and K. Tanaka.** 1985. Spectroscopic analysis of the interaction of rat liver short-chain, medium-chain, and long-chain acyl coenzyme A dehydrogenases with acyl coenzyme A substrates. Biochemistry **24:**7192–7199.
13. **Jaroszewski, L., L. Rychlewski, Z. Li, W. Li, and A. Godzik.** 2005. FFAS03: a server for profile-profile sequence alignment. Nucleic Acids Res. **33**:284–288.
14. **Jing, D., J. Agnew, W. F. Patton, J. Hendrickson, and J. M. Beechem.** 2003. A sensitive two-color electrophoretic mobility shift assay for detecting both nucleic acids and protein in gels. Proteomics **3:**1172–1180.
15. **Jones, D. T.** 1999. Protein secondary structure prediction based on position-specific scoring matrices. J. Mol. Biol. **292:**195–202.
16. **Karplus, K., R. Karchin, C. Barrett, S. Tu, M. Cline, M. Diekhans, L. Grate, J. Casper, and R. Hughey.** 2001. What is the value added by human intervention in protein structure prediction? Proteins (Suppl.) **5:**86–91.
17. **Khanna, P., and M. S. Jorns.** 2003. Tautomeric rearrangement of a dihydroflavin bound to monomeric sarcosine oxidase or *N*-methyltryptophan oxidase. Biochemistry **42:**864–869.
18. **Kim, J.-J. P., and R. Miura.** 2004. Acyl-CoA dehydrogenases and acyl-CoA oxidases. Structural basis for mechanistic similarities and differences. Eur. J. Biochem. **271:**483–493.
19. **Koh, I. Y. Y., V. A. Eyrich, M. A. Marti-Renom, D. Przybylski, M. S. Madhusudhan, N. Eswar, O. Grana, F. Pazos, A. Valencia, A. Sali, and B. Rost.** 2003. EVA: evaluation of protein structure prediction servers. Nucleic Acids Res. **31:**3311–3315.
20. **Koradi, R., M. Billeter, and K. Wüthrich.** 1996. MOLMOL: a program for display and analysis of macromolecular structures. J. Mol. Graphics Modeling **14:**51–55.
21. **Laemmli, U. K.** 1970. Cleavage of structural proteins during the assembly of the head of bacteriophage T4. Nature (London) **227:**680–685.
22. **Landini, P., L. I. Hajec, and M. R. Volkert.** 1994. Structure and transcriptional regulation of the *Escherichia coli* adaptive response gene *aidB*. J. Bacteriol. **176:**6583–6589.
23. **Landini, P., and M. R. Volkert.** 1995. Transcriptional activation of the *Escherichia coli* adaptive response gene *aidB* is mediated by binding of methylated Ada protein. J. Biol. Chem. **270:**8285–8289.
24. **Landry, J., and R. Sternglanz.** 2003. Yeast Fms1 is a FAD-utilizing polyamine oxidase. Biochem. Biophys. Res. Commun. **303:**771–776.
25. **Lenich, A. C., and S. I. Goodman.** 1986. The purification and characterization of glutaryl-coenzyme A dehydrogenase from porcine and human liver. J. Biol. Chem. **261:**4090–4096.
26. **Martinez, A., and R. Kolter.** 1997. Protection of DNA during oxidative stress by the nonspecific DNA-binding protein Dps. J. Bacteriol. **179:**5188–5194.
27. **Massey, V., and P. Hemmerich.** 1980. Active site probes of flavoproteins. Biochem. Soc. Trans. **8:**246–257.
28. **Massey, V., and P. Hemmerich.** 1978. Photoreduction of flavoproteins and other biological compounds catalyzed by deazaflavins. Biochemistry **17:**9–16.
29. **Massey, V., F. Müller, R. Feldberg, M. Schuman, P. A. Sullivan, L. G. Howell, S. G. Mayhew, R. G. Matthews, and G. P. Foust.** 1969. The reactivity of flavoproteins with sulfite. Possible relevance to the problem of oxygen reactivity. J. Biol. Chem. **244:**3999–4006.
30. **Massey, V., M. Stankovich, and P. Hemmerich.** 1978. Light-mediated reduction of flavoproteins with flavins as catalysts. Biochemistry **17:**1–8.
31. **Matsudaira, P.** 1987. Sequence from picomole quantities of proteins electroblotted onto polyvinylidene difluoride membranes. J. Biol. Chem. **262:**10035–10038.
32. **McGuffin, L. J., K. Bryson, and D. T. Jones.** 2000. The PSIPRED protein structure prediction server. Bioinformatics **16:**404–405.
33. **Miroux, B., and J. E. Walker.** 1996. Over-production of proteins in *Escherichia coli*: mutant hosts that allow synthesis of some membrane protein and globular proteins at high levels. J. Mol. Biol. **260:**289–298.
34. **Mohsen, W.-W. A., B. D. Anderson, S. L. Volchenboum, K. P. Battaile, K. Tiffany, D. Roberts, J.-J. Kim, and J. Vockley.** 1998. Characterization of molecular defects in isovaleryl-CoA dehydrogenase in patients with isovaleric acidemia. Biochemistry **37:**10325–10335.
35. **Nagpal, A., M. P. Valley, P. F. Fitzpatrick, and A. M. Orville.** 2004. Crystallization and preliminary analysis of active nitroalkane oxidase in three crystal forms. Acta Crystallogr. D Biol. Crystallogr. **60:**1456–1460.
36. **Nakajima, Y., I. Miyahara, K. Hirotsu, Y. Nishima, K. Shiga, C. Setoyama, H. Tamaoki, and R. Miura.** 2002. Three-dimensional structure of the flavoenzyme acyl-CoA oxidase II from rat liver, the peroxisomal counterpart of mitochondrial acyl-CoA dehydrogenase. J. Biochem. **131:**365–374.
37. **Nicholls, A., K. Sharp, and B. Honig.** 1991. Protein folding and association: insights from the interfacial and thermodynamic properties of hydrocarbons. Proteins Struct. Funct. Genet. **11:**281–296.
38. **Ouyang, T., and D. R. Walt.** 1991. A new chemical method for synthesizing and recycling acyl coenzyme A thioesters. J. Org. Chem. **56:**3752–3755.
39. **Rost, B.** 2001. Review: protein secondary structure prediction continues to rise. J. Struct. Biol. **134:**204–218.
40. **Sedgwick, B., and T. Lindahl.** 2002. Recent progress on the Ada response for inducible repair of DNA alkylation damage. Oncogene **21:**8886–8894.
41. **Shi, Y., F. Lan, C. Matson, P. Mulligan, J. R. Whetstine, P. A. Cole, R. A. Casero, and Y. Shi.** 2004. Histone demethylation mediated by the nuclear amine oxidase homolog LSD1. Cell **119:**941–953.
42. **Trewick, S. C., T. F. Henshaw, R. P. Hausinger, T. Lindahl, and B. Sedgwick.** 2002. Oxidative demethylation by *Escherichia coli* AlkB directly reverts DNA base damage. Nature **419:**174–178.
43. **Volkert, M. R.** 1988. Adaptive response of *Escherichia coli* to alkylation damage. Environ. Mol. Mutagen. **11:**241–255.
44. **Volkert, M. R., F. H. Gately, and L. I. Hajec.** 1989. Expression of DNA damage-inducible genes of *Escherichia coli* upon treatment with methylating, ethylating and propylating agents. Mutat. Res. **217:**109–115.
45. **Volkert, M. R., and D. C. Nguyen.** 1984. Induction of specific *Escherichia coli* genes by sublethal treatments with alkylating agents. Proc. Natl. Acad. Sci. USA **81:**4110–4114.
46. **Volkert, M. R., D. C. Nguyen, and K. C. Beard.** 1986. *Escherichia coli* gene induction by alkylation treatment. Genetics **112:**11–26.
47. **Watanabe, K., C. Khosla, R. M. Stroud, and S.-C. Tsai.** 2003. Crystal structure of an acyl-ACP dehydrogenase from the FK520 polyketide biosynthetic pathway: insights into extender unit biosynthesis. J. Mol. Biol. **334:**435–444.